STUDY OF THE PHOTO-THERMO-MECHANICAL BEHAVIOR OF PMMA-CORE POFS

D.S. Montero [(1)], J.C. Torres [(1)], J.L. Pérez-Castellanos [(2)], J. Zahr-Viñuela [(2)], C. Vázquez [(1)],

1: Electronics Technology Dpt., Universidad Carlos III de Madrid, Avda. de la Universidad 30, 28911, Leganés (Madrid), Spain.
2: Continuum Mechanics and Structural Analysis Dpt., Universidad Carlos III de Madrid, Avda. de la Universidad 30, 28911, Leganés (Madrid), Spain.

Corresponding author: dsmontero@ing.uc3m.es

Abstract: In this work, we report the results obtained during the photo-thermo-mechanical characterization of a PMMA-core plastic optical fiber (POF) through tensile tests. Simultaneous measurements of the received optical power and temperature variation during the deformation process are also reported, analyzing its viability as an intensity-based sensing system.

Key words: POF mechanical behavior, strain rate, step-index PMMA-POF, stress-strain performance.

1. Introduction

The need for accurate reliable sensors has increases because the necessity to control industrial processes and energy saving, automotive and security services. In all cases, and especially in the latter market niche which includes structural health monitoring (SHM) purposes, optical sensors have several known benefits, as they can be used in harsh and explosive environments, have a high electromagnetic compatibility, and often have a long life. Various measurands are of interest but strain is one of the most important for structural health monitoring applications. Related to standard PMMA POF fibers, they can be strained to more than 40% due to their elasto-plastic properties while fully maintaining their light guiding properties, which also make them well-suited for SHM applications when compared to FBG (Fiber Bragg Grating)-based solutions. The latter is mostly based on silica optical fiber which provides limited applications due to their low break-down strain of only percentage units of strain (typically 1%).

Different techniques employing POF for strain measurements have been reported in literature with great success. Since a Bragg grating can be written in a single mode POF [1], the POF has become an attractive optical device in sensor systems for the aforementioned applications. Nevertheless, the drawback relies on the fact that typically an Optical Spectrum Analyzers (OSA) needs to be used to monitor the wavelength shift versus strain, by its principle of operation, thus increasing the total cost of the solution employed [2]. Additionally, such POF-based FBGs also suffer from temperature dependence, becoming a constraint in applications in which temperature is seen as an external undesirable factor. In other cases, the SHM monitoring technique employs singlemode POFs extended to POF-based interferometric schemes allowing high accuracy for such measurements but increasing the complexity of the total system [3]. Finally, earlier publications have shown that distributed strain sensing with POF by evaluating the distributed Rayleigh backscatter signal using Optical Time Domain Reflectometry (OTDR) is possible [4,5].

On the other hand, and approaching simple configurations, intensity sensors modulate the optical power loss as the physical magnitude changes thus providing the measurement as an optical intensity modulation signal. In general, optical intensity sensors are very attractive since they are simple in concept, reliable, small-sized and offer a wide range of applications at lower costs, compared to other solutions. The principle of the intensity-based measurement implemented in SHM applications have been reported in literature by different authors [6-8] where in all cases the POF needed to be bent. In that cases, the fewer propagating modes experience total internal reflection at the location of the bend, and there are therefore radiated, and so the intensity of light propagated through the fiber decreases. However, simpler POF configurations with no need for fiber bending when embedding or gluing in structural elements being subjected to deformational states would be a desirable future of this kind of sensors.

The aim of this work is to demonstrate that cost-effective optical intensity-based measurements with this fiber type can be suitable as part of Structural Health Monitoring (SHM) systems beyond complex schemes. To do so, the mechanical characterization of unbent PMMA-core POF specimens through tensile tests with simultaneous measurements of the received optical power and the temperature increase due to the elastic and plastic deformations has been studied.

The paper is organized as follows: first, the theoretical background is briefly described in Section 2; next, the experimental measurements of the mechanical characterization of the PMMA-core POF are reported in Section 3; finally, the results are discussed and the conclusions are provided in Section 4.

2. Theoretical background

2.1. Refractive index vs material deformation

The mechanical deformation of a fiber consists on simultaneous axial elongation and diameter decrease. Consequently, if a ray of light propagates through the fiber, its optical path may be altered both due to the fiber elongation and the refractive index change [9-10]. Although the former can be considered having no effect in the total optical power received, a refractive index change may become of significant relevance for the light propagation through the fiber core. This effect can be attributed either to the strain suffered by the fiber either by the diameter decrease, as Eq. (1) [9] shows:

$$dn_{eq} = \frac{\partial n_{eq}}{\partial \varepsilon} d\varepsilon + \frac{\partial n_{eq}}{\partial a} \frac{\partial a}{\partial \varepsilon} d\varepsilon \tag{1}$$

being n_e the effective core refractive index, a the fiber core radius, and ε is the component of the applied strain. The first term of Eq. (1) takes into account the refractive index variation due to the applied strain, i.e. photoelastic effect whereas the second term corresponds to the refractive index change due to the fiber core radius variation. Assuming an isotropic material and neglecting the effects of both residual and tangential tensions, the refractive index change under axial strain can be written as [10]:

$$\Delta n_{eff} = -\frac{n_o^3}{2}\left\{ p_{12}\left[\varepsilon + \left(\delta + \frac{1}{2} \right)\varepsilon^2 \right] + \left(p_{11} + p_{12} \right)\left[-\nu\varepsilon + \left(\eta + \frac{\nu^2}{2} \right)\varepsilon^2 \right] \right\} \tag{2}$$

where n_o is the equivalent refractive index when no deformation is applied, p_{ij} correspond to the Pockel's constants, ν is the Poisson ratio, and δ and η are non-linear constants.

The effective refractive index variation due to core radius evolution can be estimated following the expression given in Eq. (3) from the work reported by Buck [11]:

$$b = \frac{n_e - n_2}{n_1 - n_2} \approx \frac{\left(1.1428V - 0.9960 \right)^2}{V^2} \quad ; \quad V = \frac{2\pi a}{\lambda}\sqrt{n_1^2 - n_2^2} \tag{3}$$

where b is defined as the normalized phase constant, n_1 and n_2 are the refractive indexes of the core and cladding, respectively, λ is the operating wavelength, a is the core radius now a function of the applied strain, and V is the normalized frequency. Operating on Eq. (3) it yields, where a_o is the fiber core initial radius before deformation.

$$\frac{dn_e}{da} = \frac{\lambda}{2\pi a^2}\sqrt{\frac{n_1 - n_2}{n_1 + n_2}}\left(-1.306V + 3.415 - \frac{1.984}{V} \right) \tag{4}$$

And finally:

$$a = a_0\left(1 - \nu\varepsilon + \eta\varepsilon^2 \right) \quad \Rightarrow \quad \frac{\partial a}{\partial \varepsilon} = a_0\left(-\nu + 2\eta\varepsilon \right) \tag{5}$$

where a_o is the fiber core initial radius before deformation.

2.2. Temperature increase during material deformation process

As a consequence of the deformation, a major part of the plastic work is dissipated into heat. The subsequent temperature rise induced in the material provokes a softening effect which favors potential instability as encountered notably in adiabatic shear banding phenomenon [12]. As a matter of fact, for applications involving high strain rate, e.g. high speed machining, crash, impact problems, this effect is of major interest. Nevertheless, as the PMMA refractive index shows certain degree of dependence with temperature (by means of its thermal expansion coefficient), this parameter can also play an important role when deformations are applied onto POF specimens.

$$\dot{T} - k\Delta T = -\left(\frac{E\alpha}{1-2\nu}\right)\frac{T_o \Delta Tr(\varepsilon)}{\rho C_p} + \frac{\beta}{\rho C_p}\sigma : \dot{\varepsilon}^p \tag{6}$$

where C_p stands for the heat capacity at constant pressure, ρ is the material density, k is the thermal diffusivity, α is the thermal expansion coefficient, E is the Young's modulus, ν is the Poisson's ratio and β is the Quinney-Taylor coefficient. Focusing on the second member in Eq. (6), the first term $-(E\alpha)\cdot(T_o \Delta Tr(\varepsilon))/(1-2\nu)\cdot(\rho C_p)$ represents the temperature increase due to elastic deformations (reversible) whereas the second term represents the temperature increase due to plastic deformations (irreversible). It is deduced from Eq. (6) that a material under deformation tests will decrease its superficial temperature in elastic regime; on the other hand, under plastic regime any material will increase its superficial temperature.

3. Experimental tests

For our measurements we used a standard 980µm core-diameter PMMA step index bare POF fiber with a numerical aperture of 0.47. It should be mentioned that this fiber type has a cladding with 0.01mm of thickness composed of a fluorinated polymer in order to perform light propagation condition through the fiber core.

3.1. Mechanical behavior

Quasi-static tests controlling the displacement of bare POF fiber specimens were performed. Fig. 1a shows a picture of the testing machine (INSTRON model 8516/8802) used for the deformation trials and a self-made POF specimen, respectively. It is worth mentioning that the specimen, see Fig. 1b, was especially designed in order to prevent undesirable fiber skids during the data acquisition that could distort the measurements.

(a) (b)

Fig..1.- (a) Picture of the mechanical device for strain measurements. ; (b) POF specimen.

From each test the true stress-true strain (σ-ε) relation and mechanical parameters such as Young's modulus, E, yield strength, σ_y, and the tensile strength, S_m were obtained. Statistically negligible differences between the results of different test under the same conditions were observed. Figure 2 shows the stress-strain relation obtained in a test at strain rate 0.0025 s^{-1}. The shape of the curve reveals the deformation process of the PMMA material under applied strain. Beyond the elastic limit, the first negative slope of the curve and further significant change (beyond (ε~0.1) is attributed to the reorientation of the PMMA molecular chains in the same axis of the applied load.

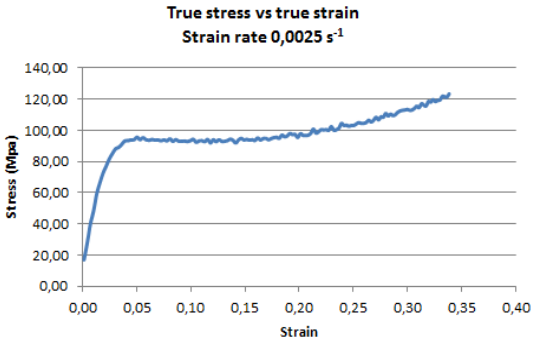

Fig.2. POF stress-strain curve, at a strain rate of 0.0025 s^{-1}.

After averaging the measured values from the different tests at strain rate 0.0025 s^{-1}, failure strain ε_{fai}=0.38, Young's modulus E_{tan} = 3850+/-75 MPa and yield stress σ_y=85-87 MPa were obtained. The tensile strength was estimated by applying the Considére criterion thus obtaining a value σ=120 MPa.

Table 1 shows the values of the Young´s modulus, yield strength, tensile strength and strain to failure obtained through tests at different strain rate. As a matter of fact, increasing the strain rate resulted in a slight increase of the Young's modulus, whereas the yield strength and the tensile strength increased significantly. In any case, by increasing the load value, the molecular chains begin to separate reaching stable relative positions that derive in permanent (plastic) deformation in the polymer.

Table 1. Summary of measured POF mechanical parameters, at different strain rates.

Strain rate	$\dot{\varepsilon} = 0,0025\ s^{-1}$	$\dot{\varepsilon} = 0,0068\ s^{-1}$
Young´s modulus MPa	3850	3930
Yield strenght MPa	85-87	105-108
Tensile strength MPa	120	150

3.2. Thermal behavior during the deformation process

A high-resolution LWIR infrared camera (model FLIR SC600) was employed to measure the temperature variations when applying different strain values onto POFs specimens. The test-bed was carefully designed to avoid undesirable heat exchange between the surface of the specimen and environment that could distort the measurements. An emissivity of 0.86 was considered for the POF fiber.

Fig. 3a shows the true stress-true strain curve obtained in a test at strain rate of 0.0072s^{-1}. On the other hand, Fig. 3b shows the corresponding temperature-true strain curve. Considering the deformation range [0.0 0.04] a decrease of (ΔT=-0.5 ºC) is noticed, as the elastic component of the deformation dominates over the plastic counterpart. Beyond de ε=0.04 the superficial temperature increases until 20.3 ºC due to the plastic component of the deformation. Figure 3b confirms that the temperature evolution is in concordance to what Eq. (6) predicts. However, POF temperature changes in deformation tests can be considered negligible due to the small measured values.

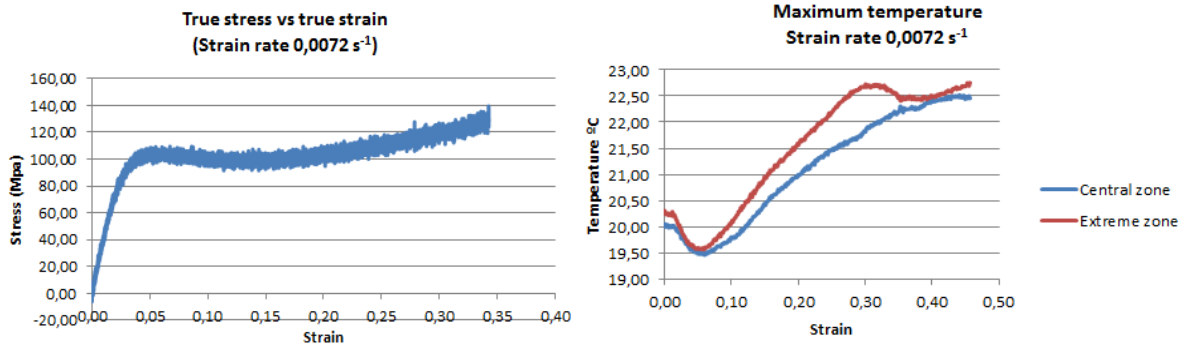

(a) (b)

Fig.3. Temperature variation suffered by a POF specimen. (a) True stress vs true strain , (b) Superficial temperature vs true strain.

3.3. Optical power behavior during the deformation process

As the main goal of this work is to demonstrate the feasibility of an unbent POF fiber acting as an intensity-based optical sensor for strain measurements, light was also launched into the POF specimens different while deformations were applied. The opto-mechanical test-bed consisted on a 635nm LED as an optical source and a photodiode with signal conditioning circuitry to provide an output voltage proportional to the detected optical power. Experimental data was recorded by means of a digital oscilloscope for an off-line signal processing. The optical power emitted by the optical source was simultaneously monitored and recorded. The experimental results obtained were calibrated with respect to the latter thus assuring self-referenced measurements.

Fig. 4 depicts the normalized average optical power received versus strain, at a strain rate of 0.0028 s^{-1} and 0.0084s^{-1}, respectively. It is clearly noticed that as the strain applied to the POF specimens increase, the received

optical power decreases. Moreover, it is shown a little influence of the applied strain rate with regards to the amount of optical power received. In both cases, upper strain limit before failure resulted in ε=0.49 in which the optical power decreased approximately 20% from the resting state, i.e. ε=0.

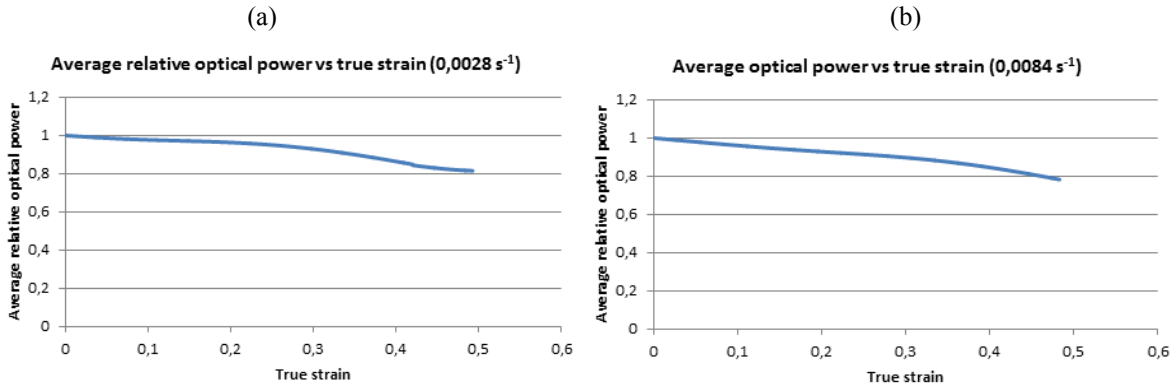

Fig. 4 Normalized received optical power versus true strain, (a) strain rate 0.0028 s^{-1} ; (b) strain rate 0.0084s^{-1}.

The optical power decrease is mainly attributed due to the POF core/cladding refractive index variation with the applied strain. Although the POF specimens were unbent, a variation of these latter parameters implies a significant change in the conditions upon light is being propagated through and optical fiber. Previous works have shown that the PMMA (core) refractive index decrease with strain whereas fluorinated polymers (cladding) increase their refractive index directly proportional to the applied strain, the latter with higher sensitivity indeed [13, 14]. Fig. 5 shows an estimation of the total loss inferred to the propagating light through the fiber for different strain values, while keeping the same launching conditions. As the critical angle ($\theta_{C)}$ is being increased more light rays will be refracted to the fiber cladding and finally attenuated thus reducing the optical power measured at reception. At resting state, and assuming refractive indexes n1=1.492 and n2=1.417 for the POF core and cladding, respectively, it results in θ_C=1.252rad. For our estimation we have considered a core/cladding refractive index change ratio of $\left|\Delta n_2 / \Delta n_1\right| = 1.5$ due to the uncertainty of the doping concentration of the POF cladding fluorinated constituents.

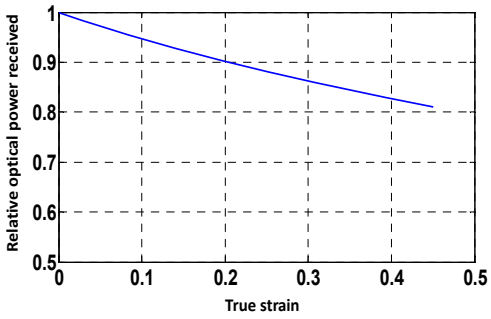

Fig. 5 Estimated optical power loss versus true strain.

4. Conclusions

We report experimental trials for bare PMMA-core POF specimens under axial strain with simultaneous measurements of the optical power detected at reception. It is clearly noticed that as the strain applied to the POF specimens increase, the received optical power decreases. To explain this effect, the main mechanical POF parameters as well as the temperature increase associated with the material deformation have been measured. The latter can be assumed to have a negligible effect on the POF core/cladding refractive index change. In contrast, remarkable strong core/cladding refractive index dependency versus the applied strain can be noticed due to the fiber constituents. This fact is assumed to be the main cause of the optical power decay, showing a quasi-linear behavior as the strain increases, and can be explained due to the change in the light propagation conditions by qualitatively analyzing the POF critical angle.

With this work we demonstrate that cost-effective optical intensity-based measurements with this fiber type can be suitable as part of Structural Health Monitoring (SHM) systems beyond complex schemes with even no need for fiber bending when embedding or gluing in structural elements being subjected to deformational states.

Acknowledgements

This work has been sponsored by the Spanish Ministries of Economy and Education (grants nº TEC2012-37983-C03-02 and Ref. PRX12/00007).

References

[1] Z. Xiong. G.D. Peng, B. Wu, P.L. Chu, *"Highly Tunable Bragg Gratings in single-Mode Polymer Optical Fibers"*, IEEE Phot. Tech. Lett., 11(3), 352-354, 1999.

[2] D. Barrera, G. Muñoz, S. Sales, *"Design, fabrication and characterization of a sensor for large strain measurement based on POFBGs"*, Reunión Nacional Española de Optoelectrónica, pp. 79-82, 2013.

[3] S. Kiesel, K. Peters, O. Abdi, T. Hassan, M. Kowalsky, *"Polymer optical fiber sensors for civil infrastructure systems"*, Proc. SPIE Sensors and Smart Structures technologies for Civil, Mechanical and Aerospace Systems, vol. 6529, paper 65293B, 2007.

[4] K. Nakamura, I.R. Husdi, S. Ueha, *"A distributed strain sensor with the memory effect based on the POF OTDR"*, Proc. SPIE International Conference on Optical Fibre Sensors, 5855, pp. 807-801, 2005.

[5] S. Liehr, P. Lenke, K. Krebber, M. Seeger, E. Thiele, H. Metschies, B. Gebreselassie, J.C. Münich, L. Stempniewski *"Distributed strain measurement with polymer optical fibers integrated into multifunctional geotextiles"*, in Proc. SPIE Optical Sensors, vol. 7003, paper 700302, 2008.

[6] K.S.C. Kuang, W.J. Cantwell, C. Thomas, "Crack detection and vertical deflection monitoring in concrete beams using plastic optical fibre sensors", Meas. Sci. Technol., 14, 205-216, 2003.

[7] N. Takeda, "Characterization of microscopic damage in composite laminates and real-time monitoring by embedded optical fibre sensors", International Journal of Fatigue, 24, 281-289, 2002.

[8] K.S.C. Kuang, W.J. Cantwell, "The use of plastic optical fibres and shape memory alloys for damage assesment and damping control in composite materials", Meas. Sci. Technol., 13, 1305-1313, 2003.

[9] C.D. Butter, G.B. Hocker, *"Fiber optics strain gauge"*, Appl. Opt., 17(18), 2867-2869, 1978.

[10] R.J. van Steenkiste, G.S. Springer, *"Strain and temperature measurement with fiber optic sensors"*, Lancaster, PA, Technomic Publishing, 1997.

[11] J.A. Buck, *"Fundamentals of optical fibers"*, Wiley&Sons, Inc., 2004.

[12] P. Lóngere, A. Gragon, "Evaluation of the inelastic heat fraction in the context of microstructure-supported dynamic plasticity modelling", International Journal of Impact Engineering, 35(9), 992-999, 2008.

[13] M.A. Silva-López, W.N. Fender, W.N. MacPherson, J.S. Barton, J.D.C Jones, D. Zhao, D.J. Webb, L. Zhang, I. Bennion, *"Strain and temperture sensitivity of a singlemode polymer optical fibre"*, Opt. Lett., 30(23), 3129-3131, 2005.

[14] Asahi Glass CYTOP data sheet, available online at http://www.agc.com/english/chemicals/shinsei/cytop/about.html.